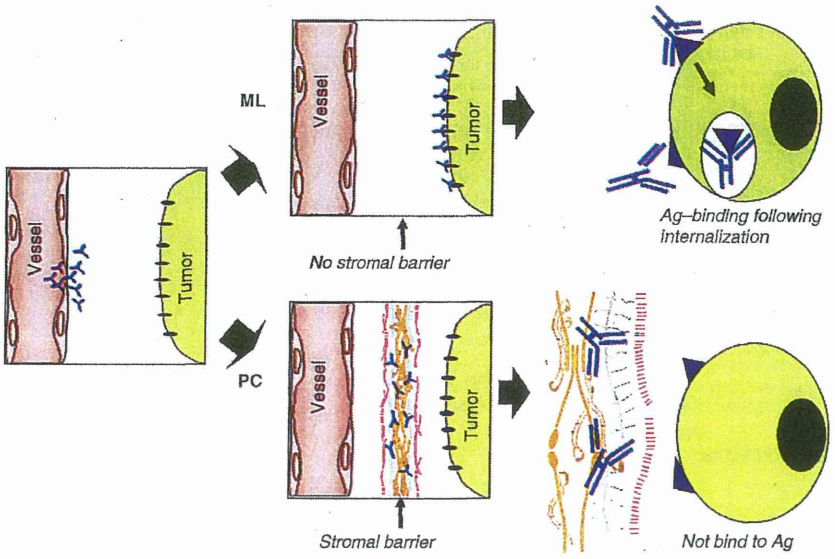

Fig. 6.1 The schema of antibody delivery into the tumor cells. In the tumor having no stromal barrier like malignant lymphoma (ML), antibodies were delivered into the cancer cells, can be internalized after antigen-binding. However, many human solid tumors including pancreatic cancer (PC) possess stromal barrier hindering the distribution of the immunoconjugates into cancer cells such that antigen-binding following antibody-intrernalization never occur. Ag, Antigen

such annoying characteristics of cancer cells themselves, most human solid tumors such as pancreatic cancer and gastric cancer possess abundant stroma that hinders the distribution of mAbs (Fig. 6.1) [25–28]. To overcome these drawbacks, we developed a unique strategy that the cancer stromal targeting (CAST) therapy by cytotoxic immunoconjugate bound to the collagen IV or fibrin network in the tumor stroma from which the payload is released gradually and distributed throughout the tumor, resulting in the arrest of tumor growth due to induced damage to tumor cells and tumor vessels [29, 30]. However, the merit and demerit of anti-stromal targeting immunoconjugate therapy in relation to the conjugate design and the amount of tumor stroma were not yet fully elucidated.

In this context, it is important to clarify the appropriate combination of targeting antibody and conjugate design of antitumor immunoconjugate depending on a quantity of tumor stroma. Hence, we selected two types of conjugate linker, ester bond and carbamate bond. We hypothesized that combination of anti-stromal targeting mAb and a linker composed of ester bond to release ACA outside the cells would be effective against the stroma-rich cancer. Conversely, anticancer cell targeting via carbamate bond to release ACA inside the cells would be effective against stroma-poor cancer. It seemed that outcome of immunoconjugate therapy against each individual tumor having distinct stromal structure was dependent on the selection of conjugation design, as well as targeting mAb.

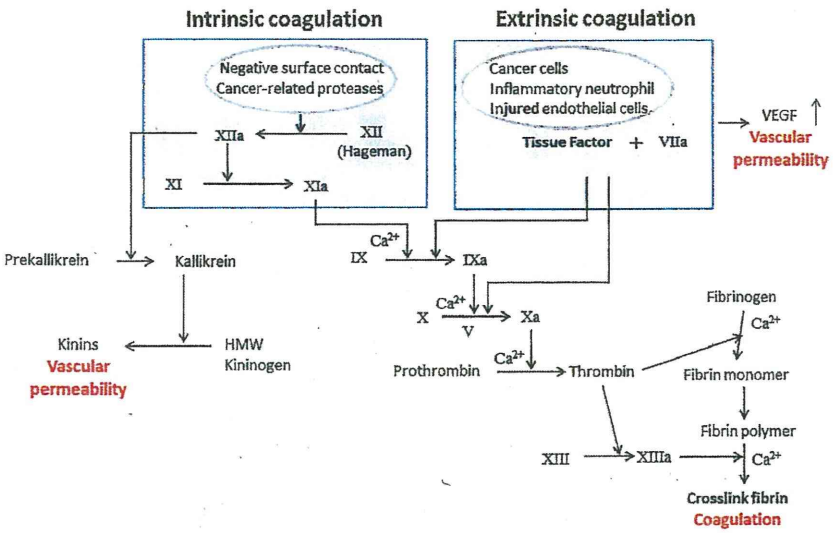

Fig. 6.2 Tumor-induced blood coagulation cascade. Both intrinsic and extrinsic coagulation factors may be involved in tumor vascular permeability

Cancer Stroma

The increased tumor vascular permeability is the most important event for the EPR effect. At the time we proposed the EPR effect, we also succeeded in purifying two types of kinin (bradykinin and hydroxyprolyl^3-bradykinin) from the ascitic fluid of a patient with gastric cancer [1, 31]. We also clarified that this kinin generation system was triggered by the activated Hageman factor, an intrinsic coagulation factor XII [32].

Meanwhile, Dvorak et al. discovered that vascular permeability factor (VPF) was involved in tumor vascular permeability [33]. Later, it was found that VPF was identical to vascular endothelial growth factor (VEGF) [34]. Recently, an extrinsic coagulation factor, namely a tissue factor (TF), appeared to activate VEGF production [35]. So, both intrinsic and extrinsic coagulation factors may be involved in tumor vascular permeability as well as tumor-induced blood coagulation (Fig. 6.2).

In the nineteenth century, French surgeon Armand Trousseau described thrombophlebitis in patients with stomach cancer for the first time [36]. Today, a large body of clinical evidence supports the conclusion that abnormal coagulation occurs in a variety of cancer patients [37]. It is now known that TF is highly expressed on the surface of almost all human cancer cells, and alternatively spliced soluble TF is also produced by many types of tumor [35]. Therefore, TF may be involved in tumor-related abnormal blood coagulation.

Above all, any malignant tumor can erode the surrounding normal tissue, and the more erosive types of cancer have more destructive actions. If these cancer clusters erode adjacent normal or tumor vessels, microscopic hemorrhage may occur at any

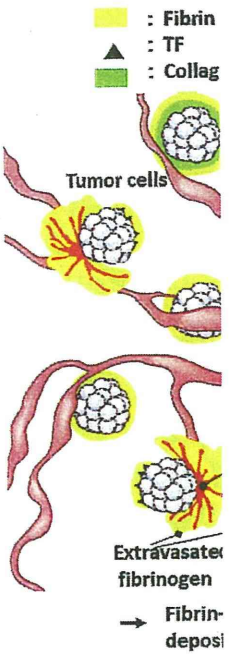

Fig. 6.3 A diagram of the

place and at any time
ately form in situ to st
collagenous stroma in
nonmalignant diseases
diac infarction, brain i
only at the onset or a
digestion or replacem
some symptoms. On t
long as the cancer cel
this "malignant cycle
metastasis progress v
needed). When any sy
tion, or macroscopic b
and destruction of the
of a particular place
cancer receive chemot
patients if they suffer
injury, or active infla

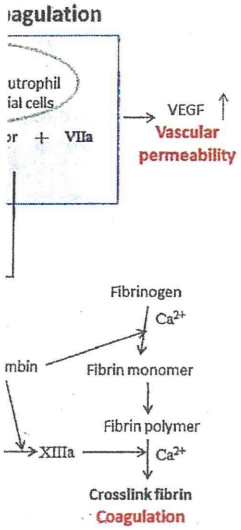

and extrinsic coagulation

rtant event for the EPR
ceeded in purifying two
from the ascitic fluid of
it this kinin generation
trinsic coagulation fac-

ability factor (VPF) was
is found that VPF was
. Recently, an extrinsic
activate VEGF produc-
ors may be involved in
l coagulation (Fig. 6.2).
sseau described throm-
ne [36]. Today, a large
mal coagulation occurs
is highly expressed on
ly spliced soluble TF is
TF may be involved in

g normal tissue, and the
If these cancer clusters
rhage may occur at any

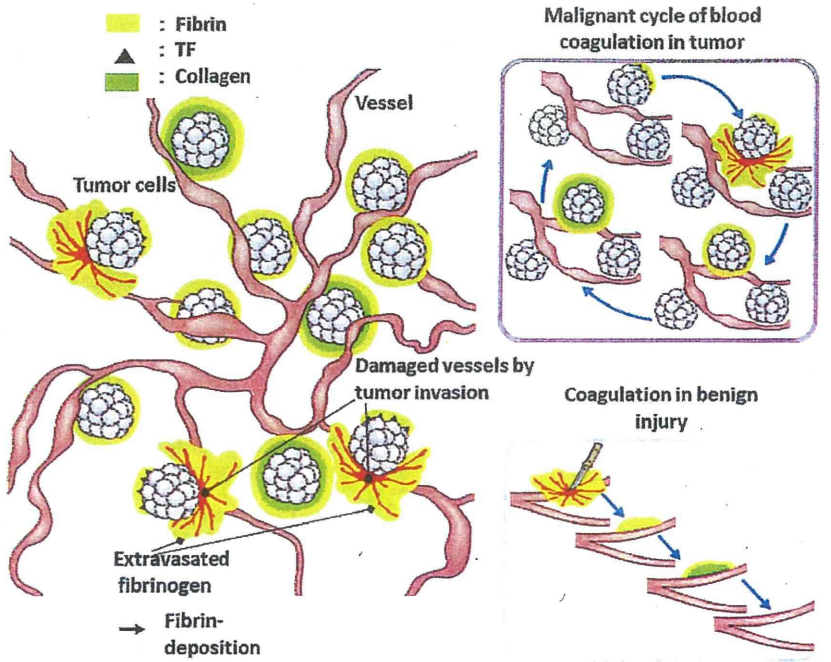

Fig. 6.3 A diagram of the 'malignant cycle of blood coagulation' in cancer tissue

place and at any time within or adjacent to cancer tissues, and fibrin clots immediately form in situ to stop the bleeding. The fibrin clots are subsequently replaced by collagenous stroma in a process similar to that in normal wound healing and other nonmalignant diseases. Fibrin clot formation in nonmalignant disorders such as cardiac infarction, brain infarction, injuries, and active rheumatoid arthritis should form only at the onset or active state of disease and subsequently disappear by plasmin digestion or replacement with collagen within a few weeks and is accompanied by some symptoms. On the other hand, the fibrin clot formation in cancer lasts for as long as the cancer cells survive in the body and occurs silently. Therefore, we call this "malignant cycle of blood coagulation" (Fig. 6.3). In fact, tumor invasion and metastasis progress without symptoms (which is why imaging instruments are needed). When any symptoms accompanying cancer such as pain, intestinal obstruction, or macroscopic bleeding occur, the cancer is likely to involve the sensory nerves and destruction of the bones and larger blood vessels and to occupy the whole lumen of a particular place of the intestine. Usually, patients with an advanced stage of cancer receive chemotherapy and it is worth noting that oncologists never treat such patients if they suffer from existing acute thrombotic complications, bleeding by injury, or active inflammation. Therefore, we conclude that cancer-induced blood

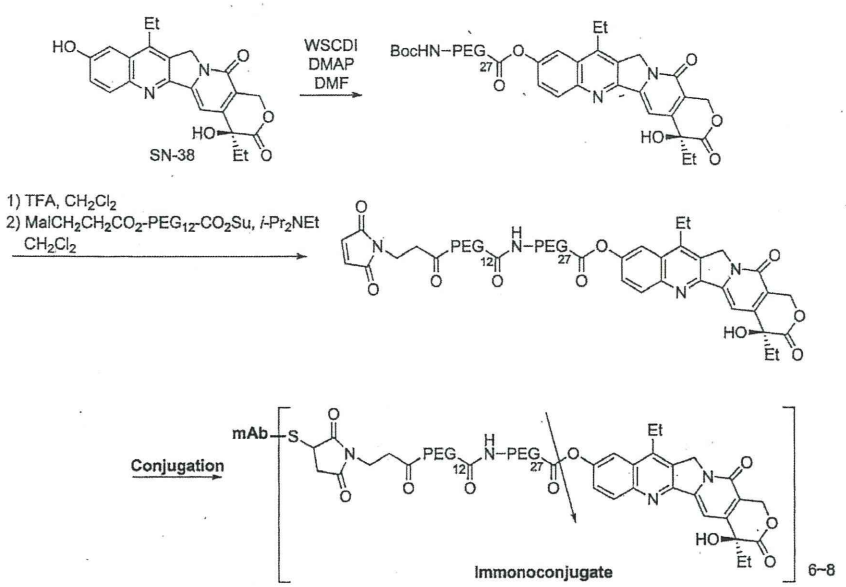

Fig. 6.4 Synthetic scheme of the immunoconjugate. The arrow indicates the cleavage site for releasing free active SN-38. PEG, Polyethylene glycol

coagulation may be an origin of tumor stroma and that fibrin clots in cancer tissues of patients who can receive chemotherapy are actually tumor specific.

CAST Therapy

CAST Therapy Using Anti-collagen 4 mAb

SN-38 is a topoisomerase 1 inhibitor and an active component of CPT-11 which is used clinically for colorectal, lung, and other cancers. For the mAb conjugation to phenol-OH in SN-38, an ester bond was selected. In our design, polyethylene glycol (PEG) was combined close to the bond (Fig. 6.4). PEG is known to evade nonspecific capture by RES. The drug (SN-38)/mAb ratio (the number of drugs attached to a mAb) of each immunoconjugate ranged from 6.7 to 8.4.

Antitumor activities of immunoconjugates with ester bond SN-38 were evaluated in mice bearing human pancreatic tumor genografts. CPT-11 and three immunoconjugates showed significant antitumor activities compared to results in mice treated with saline, in mice bearing either PSN1 (EpCAM positive and stroma poor) or SUIT2 (EpCAM positive and stroma rich) tumors. In SUIT2 tumors, while the tumor continued to increase in mice treated with CPT-11, anti-CD20 immunoconjugate (as a nonspecific control), and anti-EpCAM immunoconjugate, the tumor in

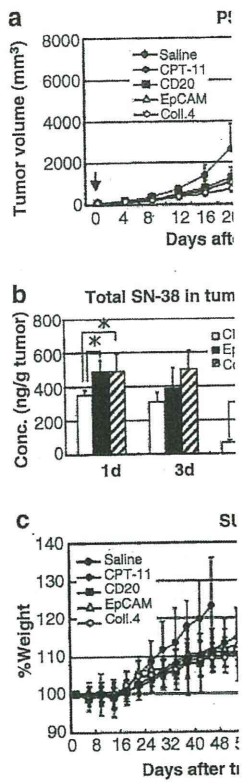

Fig. 6.5 Anti-tumor effect
lagen 4 immunoconjugate
PSN1 and SUIT2, the 3 i
groups of mice by intrave
the curves illustrate the e
EpCAM in PSN1), P<0.01
in SUIT2), P<0.001 (Salin
or EpCAM vs. Collagen 4
and unbound) SN-38 (up
(lower) were determined u
*P<0.05, Bar=SD. (c) Ch
Collagen 4 in the same tr
change of jejunum from n
(lower). Scale bar: 1mm. (

mice treated with anti
month and never resur
(stroma poor), differe
38 immunoconjugate
anti-CD20 or anti-Ep

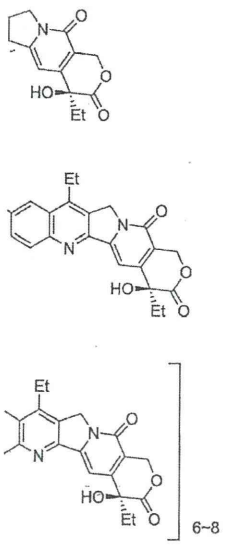

6~8

ates the cleavage site for

clots in cancer tissues
specific.

nt of CPT-11 which is
e mAb conjugation to
n, polyethylene glycol
own to evade nonspe-
er of drugs attached to

ıd SN-38 were evalu-
T-11 and three immu-
red to results in mice
itive and stroma poor)
IT2 tumors, while the
-CD20 immunoconju-
ɔnjugate, the tumor in

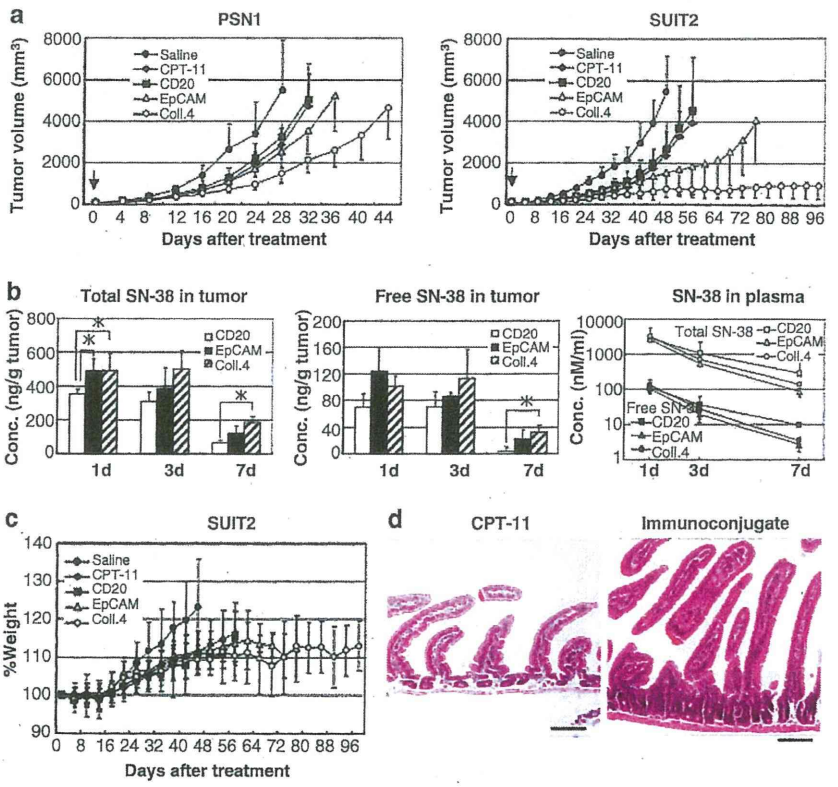

Fig. 6.5 Anti-tumor effects, pharmacokinetics and drug toxicities of anti-CD20, EpCAM and collagen 4 immunoconjugates. (**a**) Anti-tumor activities in vivo were examined. In animal models of PSN1 and SUIT2, the 3 immunoconjugates or saline as control, were administered to separate groups of mice by intravenous bolus injection on day. Arrows indicate day of administration and the curves illustrate the effects of the treatments on tumour size. P<0.05 (Saline or CD20 vs. EpCAM in PSN1), P<0.01 (Saline vs. CPT11 or EpCAM in PSN1, CPT11 or CD20 vs. EpCAM in SUIT2), P<0.001 (Saline vs. CPT11 or CD20 or EpCAM in SUIT2, Saline or CPT11 or CD20 or EpCAM vs. Collagen 4 in PSN1 or SUIT2). Bar=SD. (**b**) Tumor concentrations of total (bound and unbound) SN-38 (upper) and free (unbound) SN-38 (middle), and plasma concentrations (lower) were determined using HPLC analysis. The concentrations on days 1, 3 and 7 are shown. *P<0.05, Bar=SD. (**c**) Changes in the % body weight of saline, CPT-11, CD20, EpCAM and Collagen 4 in the same treated SUIT2 group (A) were shown Bar = SD. (**d**) Pathologic mucosal change of jejunum from mouse treated with CPT11 (upper) or anti-collagen 4 immunoconjugate (lower). Scale bar: 1mm. Coll.4,Collagen 4; Conc.,Concentration

mice treated with anti-collagen IV immunoconjugate stopped growing by about 1 month and never resumed up to 3 months (Fig. 6.5a). In mice bearing PSN1 tumors (stroma poor), differences were present but less marked. Thus, anti-collagen 4-SN-38 immunoconjugate exerted the most potent antitumor activity as compared with anti-CD20 or anti-EpCAM immunoconjugates and CPT-11 (Fig. 6.5a). In both

tumor models, anti-EpCAM immunoconjugate exerted superior antitumor effect compared to CPT-11 and anti-CD20 immunoconjugate, but inferior antitumor effect to anti-collagen IV immunoconjugate.

Significantly higher concentrations of free and total SN-38 were detected in tumor tissues of mice treated with the anti-collagen 4 immunoconjugate compared to the anti-CD20 immunoconjugate (Fig. 6.5b). The concentration of free and SN-38 in the tumor treated with anti-EpCAM immunoconjugate was intermediate among them, but not significant (Fig. 6.5b). There was no significant difference in body weight changes among saline groups, CPT-11, and immunoconjugate groups (Fig. 6.5c). In the small intestinal mucosa of mice, widespread villous atrophy and decreased crypt density were observed by the treatment of free unbound CPT-11 which is well known to have severe intestinal toxicity in clinics. On the other hand, the small intestinal mucosa of mice in groups treated with all immunoconjugates did not show any pathological change (Fig. 6.5d).

The most important observation from a therapeutic standpoint was that only SUIT2 tumors treated with anti-collagen IV immunoconjugate stopped growing about 1 month after treatment and remained dormant for more than 3 months. It may be concluded that the strategy of orchestrating slow sustained release from a scaffold erected on the stable inert structural components of the tumor stroma is most effective. We histologically compared this nongrowing tumor with a size-matched, growing, control tumor and found that both tumors showed central necrosis due to decreased blood flow, which is often observed in a murine xenotransplant model [38, 39]. The striking difference was that large confluent necrotic zones and dense fibrotic capsule formation were observed only in the treated tumor (Fig. 6.6a, b). In addition, CD31-positive endothelial cells, which may be tumor-feeding vessels in the peripheral part of the tumor, were never observed in the treated tumor compared with the untreated control. Instead, many collagen 4-positive round profiles corresponding to traces of destroyed vessels were observed in the peripheral area of the treated tumor (Fig. 6.6c).

CAST Therapy Using Anti-fibrin mAb

Chemically induced mouse cutaneous cancer was selected as an appropriate experimental model for evaluating the therapeutic effects of our immunoconjugate chemotherapy, because this spontaneous carcinogenetic model has remarkable fibrin deposition and abundant interstitial tissue as in human cancer (Fig. 6.7a), unlike human tumor xenografts, which have less fibrin clots and interstitial tissue [40, 41]. In addition, the spontaneous tumor is very slow in tumor growth that is also more similar to the general human cancer as compared to the xenografts. Using systemic in vivo imaging, anti-fibrin IgM, anti-fibrin chimeric IgG, and anti-fibrinogen IgG were delivered and retained in the tumor until day 3, utilizing leaky tumor vessels [1–3]. However, accumulation of anti-fibrin IgM and anti-fibrinogen IgG was weak

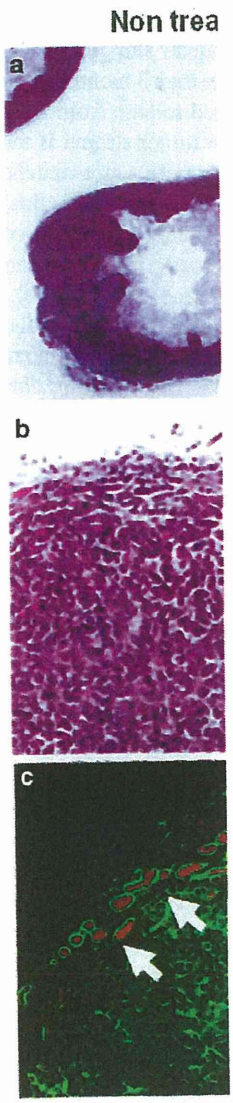

Fig. 6.6 Histopathologic
ment.(a) Hematoxylin an
SUIT2-tumors. A non-ne
The fibrotic capsule widt
vessels were examined b
arrows indicate tumor ves

iperior antitumor effect
inferior antitumor effect

iN-38 were detected in
unoconjugate compared
icentration of free and
jugate was intermediate
significant difference in
imunoconjugate groups
ead villous atrophy and
f free unbound CPT-11
nics. On the other hand,
i all immunoconjugates

andpoint was that only
jugate stopped growing
re than 3 months. It may
ied release from a scaf-
ie tumor stroma is most
ior with a size-matched,
l central necrosis due to
e xenotransplant model
ecrotic zones and dense
l tumor (Fig. 6.6a, b). In
umor-feeding vessels in
treated tumor compared
ve round profiles corre-
ie peripheral area of the

is an appropriate experi-
immunoconjugate che-
el has remarkable fibrin
ncer (Fig. 6.7a), unlike
terstitial tissue [40, 41].
growth that is also more
iografts. Using systemic
and anti-fibrinogen IgG
ing leaky tumor vessels
ibrinogen IgG was weak

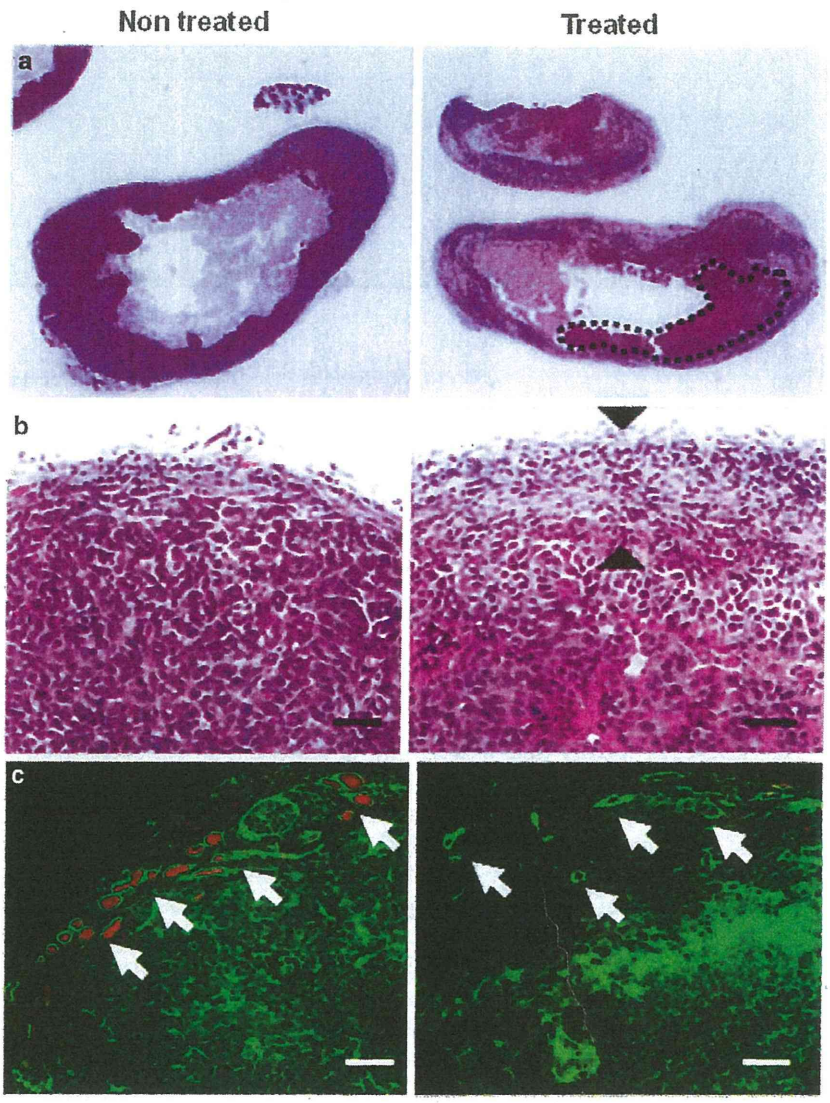

Fig. 6.6 Histopathological features of SUIT2 tumors after anti-collagen 4 immunoconjugate treatment.**(a)** Hematoxylin and eosin staining of non-treated (left) and immunoconjugate-treated (right) SUIT2-tumors. A non-necrotic viable lesion in the treated tumor is enclosed by a dotted line. **(b)** The fibrotic capsule width in the treated tumor is indicated between black arrowheads. **(c)** Tumor vessels were examined by the CD31 (red) collagen IV (green) double-staining techniques. White arrows indicate tumor vessels or their traces in the boundary area. Scale bar: 100μm

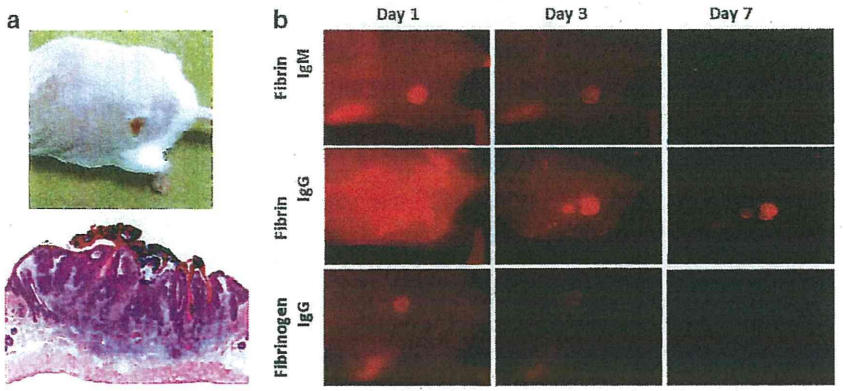

Fig. 6.7 (**a**) Chemical skin carcinogenesis. Mouse bearing a tumor (upper) and hematoxylin-eosin staining (lower) were shown. (**b**) In vivo systemic imaging analysis of Alexa-647-labeled anti-fibrin IgM (upper), Anti-fibrin chimeric mAb (middle) or anti-fibrinogen mAb (lower) on Days 1, 3 and 7 after injection. Arrows indicate each tumor position

and was eliminated by day 7, but the chimeric IgG was still highly retained (Fig. 6.7b). The use of human chimera is beneficial for clinical application to avoid human anti-mouse neutralizing antibodies (HAMA) and allergic reaction in human. In addition, because of the rapid blood clearance and low penetration of IgM compared with IgG [42], IgM is not suitable as a drug delivery vehicle. The branched composition had one maleimide for attachment of mAb, one PEG_{12} spacer, and three PEG_{27} ester bonds for attachment of three SN-38 molecules (Fig. 6.8a). There were approximately eight thiol residues able to react with the maleimide in the reduced mAb. The calculated drug (SN-38)/mAb ratio of the immunoconjugate was about 24. This immunoconjugate exerted significantly stronger antitumor activity compared with CPT-11 (Fig. 6.8b). Although treatment-related body weight loss was observed in mice treated with each drug, there was no significant difference between control groups and CPT-11 or the immunoconjugate treatment group. After injection of the immunoconjugate, the concentration of total SN-38 (antibody bound and unbound form) and free SN-38 (unbound form) in plasma gradually declined within a week, whereas CPT-11 showed rapid clearance (Fig. 6.9a). Significantly high concentrations of total and free SN-38 were detected in tumor tissues treated with the immunoconjugate for a long time compared to CPT-11 (Fig. 6.9b). The second significant observation of the treatment was a change in the gross tumor color from reddish to white (Fig. 6.9c). There was no clear change of fibroblast or macrophage, which plays an important role for tumor progression [43, 44]. It was found that discontinuation and irregularity comprising a mixture of narrowness and enlargement of the tumor vessels were manifested after treatment with the immunoconjugate (Fig. 6.9d, e).

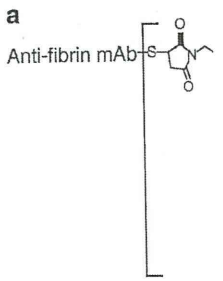

Fig. 6.8 Drug design, ant
immunoconjugate; anti-fibi
body bears 24 molecules o
SN-38. (**b**) Anti-tumor ac
were administered to mice
on Day 0, 7, 14, and 21. Ar
of treatment on tumor size
immunoconjugate). Bar =

We have made clea
immunoconjugate. Ou
apy is unique as follow

1. Newly developed c
tumor vessels select
mal network.
2. The immunoconjug
from the scaffold, a
tumor.

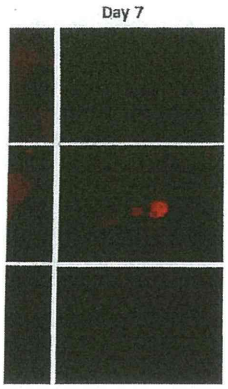

er) and hematoxylin-eosin
f Alexa-647-labeled anti-
n mAb (lower) on Days 1,

still highly retained
al application to avoid
gic reaction in human.
netration of IgM com-
vehicle. The branched
ne PEG_{12} spacer, and
ules (Fig. 6.8a). There
the maleimide in the
immunoconjugate was
ger antitumor activity
ated body weight loss
significant difference
treatment group. After
N-38 (antibody bound
ma gradually declined
g. 6.9a). Significantly
1 tumor tissues treated
T-11 (Fig. 6.9b). The
ge in the gross tumor
change of fibroblast or
ession [43, 44]. It was
ure of narrowness and
nent with the immuno-

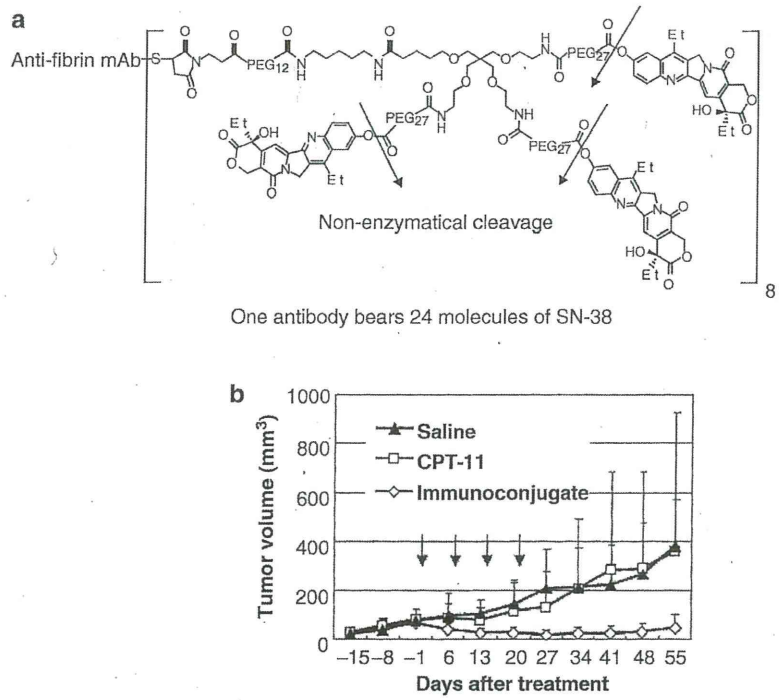

Fig. 6.8 Drug design, anti-tumor effect of anti-fibrin immunoconjugate (**a**) Drug design of immunoconjugate; anti-fibrin mAb-PEG-three branched PEG-(SN-38)3 via ester bond. One antibody bears 24 molecules of SN-38. The arrow indicates the cleavage site for releasing free active SN-38. (**b**) Anti-tumor activity in vivo was examined. Immunoconjugates, CPT-11 or saline, were administered to mice bearing chemical-induced cutaneous cancer via intravenous injection on Day 0, 7, 14, and 21. Arrows indicate day of administration and the curves illustrate the effect of treatment on tumor size. P =0.0005 (CPT-11 vs. immunoconjugate), P < 0.0001 (saline vs. immunoconjugate). Bar = SD

We have made clear that our newly developed tool is not a simple cytotoxic immunoconjugate. Our strategic concept of cancer stromal targeting (CAST) therapy is unique as follows.

1. Newly developed cytotoxic immunoconjugate can extravasate from the leaky tumor vessels selectively and forms a scaffold as it is captured by the tumor stromal network.
2. The immunoconjugate allows the effective sustained release of anticancer agent from the scaffold, and this released anticancer agent is distributed throughout the tumor.

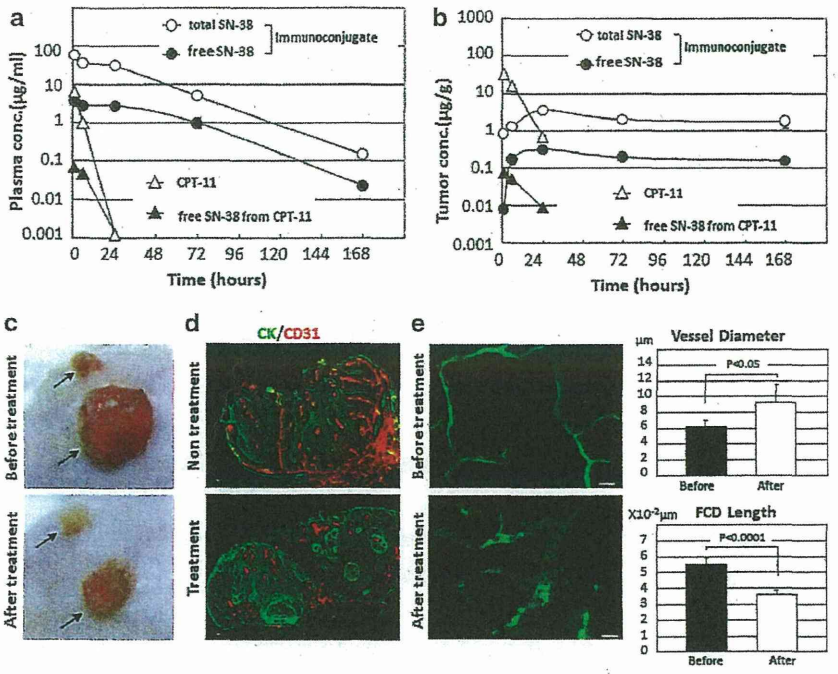

Fig. 6.9 Drug distribution and anti-vascular activity of anti-fibrin mAb conjugated with SN-38 (**a**) Plasma concentration of total SN-38 (bound and unbound form) or CPT-11 and free SN-38 (unbound form) released from the immunoconjugate or converted from CPT-11 was determined using HPLC analysis 1, 6, 24, 72, and 168 h after the injection. (**b**) Tumor concentration of total SN-38 (bound and unbound form) and free SN-38 (unbound form) released from the immunoconjugate, CPT-11 and free SN-38 converted from CPT-11 was determined using HPLC. (**c**) Tumor color changed from reddish to white at 5 days after injection of the immunoconjugate but not CPT-11. Arrows indicate each tumor position. (**d**) Tumor vessels after the injection of the immunoconjugate (Treatment) were examined using CD31 (red) and CK (cytokeratin, green). Untreated mouse (Non treatment) was used as control. bar: 100 μm. (**e**) Tumor vessels before and after the injection were visualized using FITC-dextran by in vivo fibered confocal fluorescence microscopy (left). Quantified vessel diameter and functional capillary density (FCD) length are shown (right). Bar: 20 μm

Consequently, the strategy described above was highly effective in causing arrest of tumor growth due to induced damage to tumor cells and tumor vessels without exerting the drug adverse effect (Fig. 6.10). Cancer stromal targeting therapy, utilizing a cytotoxic agent conjugated to a mAb directed at a specific inert constituent of the tumor stroma, is thus validated as a highly effective new modality of oncological therapy [45].

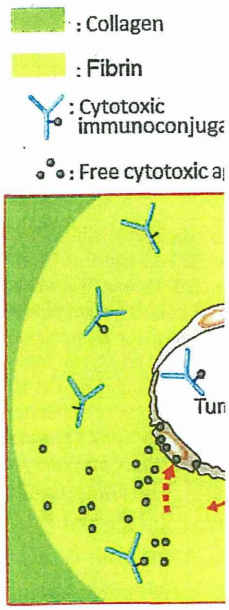

Fig. 6.10 Diagram of nev
oped anti-fibrin mAb cor
bind specifically to the fib
the effective sustained rel
Since this released anti-ca
stroma barrier and induce

Tailored ADC De

Difference of Tun Lymphoma and P

Anti-collagen 4 mAb
malignant lymphoma
collagen-4-positive b
spersed fibrously like
tumor, SUIT2 tumor
human pancreatic car
collagen-4-positive e
CD31-positive blood